

## Article

# The First-In-Class Anti-AXL × CD3ε Pronectin™-Based Bispecific T-Cell Engager Is Active in Preclinical Models of Human Soft Tissue and Bone Sarcomas

Nicoletta Polerà <sup>1,†</sup>, Antonia Mancuso <sup>1,†</sup> , Caterina Riillo <sup>1</sup>, Daniele Caracciolo <sup>1</sup>, Stefania Signorelli <sup>1</sup>, Katia Grillone <sup>1</sup> , Serena Ascrizzi <sup>1</sup>, Craig A. Hokanson <sup>2</sup>, Francesco Conforti <sup>3</sup>, Nicoletta Staropoli <sup>1</sup>, Luigia Gervasi <sup>1</sup>, Maria Teresa Di Martino <sup>1</sup> , Mariamena Arbitrio <sup>4</sup> , Giuseppe Nisticò <sup>5</sup>, Roberto Crea <sup>2,5</sup>, Pierosandro Tagliaferri <sup>1</sup>, Giada Juli <sup>1,\*</sup>  and Pierfrancesco Tassone <sup>1,6,\*</sup> 

<sup>1</sup> Department of Experimental and Clinical Medicine, Magna Græcia University, 88100 Catanzaro, Italy

<sup>2</sup> Protelica, Inc., Hayward, CA 94545, USA

<sup>3</sup> Pathology Unit, Annunziata Hospital, 87100 Cosenza, Italy

<sup>4</sup> Institute of Research and Biomedical Innovation (IRIB), Italian National Council (CNR), 88100 Catanzaro, Italy

<sup>5</sup> Renato Dulbecco Institute, 88046 Lamezia Terme, Italy

<sup>6</sup> College of Science and Technology, Temple University, Philadelphia, PA 19122, USA

\* Correspondence: giadajuli@libero.it (G.J.); tassone@unicz.it (P.T.)

† These authors contributed equally to this work.

‡ These authors contributed equally to this work.

**Simple Summary:** Sarcomas are a group of heterogeneous diseases with a poor prognosis and scarce therapeutic options. Innovative approaches based on novel therapeutic targets are eagerly awaited. AXL, a TAM family tyrosine kinase receptor, recently emerged as an interesting target for several type of sarcomas. Here, we propose an innovative immunotherapeutic strategy based on the targeting of AXL, using a first-in-class Pronectin™-based Bispecific T-Cell Engager (pAXL × CD3ε) for the treatment of sarcomas. Our results demonstrate that pAXL × CD3ε redirects T cells toward AXL-expressing sarcoma cell lines, leading a dose-dependent and T cell-mediated cytotoxicity in vitro. Moreover, pAXL × CD3ε inhibits the in vivo growth of human sarcoma xenografts and improves survival in immunocompromised mice, thus representing a new-generation strategy for the treatment of a still-incurable disease.

**Abstract:** Sarcomas are heterogeneous malignancies with limited therapeutic options and a poor prognosis. We developed an innovative immunotherapeutic agent, a first-in-class Pronectin™-based Bispecific T-Cell Engager (pAXL × CD3ε), for the targeting of AXL, a TAM family tyrosine kinase receptor highly expressed in sarcomas. AXL expression was first analyzed by flow cytometry, qRT-PCR, and Western blot on a panel of sarcoma cell lines. The T-cell-mediated pAXL × CD3ε cytotoxicity against sarcoma cells was investigated by flow cytometry, luminescence assay, and fluorescent microscopy imaging. The activation and degranulation of T cells induced by pAXL × CD3ε were evaluated by flow cytometry. The antitumor activity induced by pAXL × CD3ε in combination with trabectedin was also investigated. In vivo activity studies of pAXL × CD3ε were performed in immunocompromised mice (NSG), engrafted with human sarcoma cells and reconstituted with human peripheral blood mononuclear cells from healthy donors. Most sarcoma cells showed high expression of AXL. pAXL × CD3ε triggered T-lymphocyte activation and induced dose-dependent T-cell-mediated cytotoxicity. The combination of pAXL × CD3ε with trabectedin increased cytotoxicity. pAXL × CD3ε inhibited the in vivo growth of human sarcoma xenografts, increasing the survival of treated mice. Our data demonstrate the antitumor efficacy of pAXL × CD3ε against sarcoma cells, providing a translational framework for the clinical development of pAXL × CD3ε in the treatment of human sarcomas, aggressive and still-incurable malignancies.

**Keywords:** sarcomas; AXL; pronectins™; bispecific T-cell engager; BTCE; immunotherapy; cancer



**Citation:** Polerà, N.; Mancuso, A.; Riillo, C.; Caracciolo, D.; Signorelli, S.; Grillone, K.; Ascrizzi, S.; Hokanson, C.A.; Conforti, F.; Staropoli, N.; et al. The First-In-Class Anti-AXL × CD3ε Pronectin™-Based Bispecific T-Cell Engager Is Active in Preclinical Models of Human Soft Tissue and Bone Sarcomas. *Cancers* **2023**, *15*, 1647. <https://doi.org/10.3390/cancers15061647>

Academic Editor: Catrin Sian Rutland

Received: 13 February 2023

Revised: 3 March 2023

Accepted: 5 March 2023

Published: 8 March 2023



**Copyright:** © 2023 by the authors. Licensee MDPI, Basel, Switzerland. This article is an open access article distributed under the terms and conditions of the Creative Commons Attribution (CC BY) license (<https://creativecommons.org/licenses/by/4.0/>).

## 1. Introduction

Sarcomas are a large group of heterogeneous malignancies of mesenchymal origin, commonly characterized by a poor prognosis, of which the onset may occur at any age [1,2]. Among them, soft tissue sarcomas (STSs) represent 80%, bone sarcomas 15% and gastrointestinal stromal tumors 5%. Because of their heterogeneity and common aggressive nature, they are resistant to available therapies and clinical management is still highly challenging [3–5]. Conventional treatment, including surgery, radiation therapy and chemotherapy (Doxorubicin, Ifosfamide, trabectedin, and others), differs from one subtype to another. Surgery is the first-line treatment for localized sarcomas, in combination with pre- or post-operative therapies [6], while chemotherapy is the standard treatment for metastatic disease. Unfortunately, the median survival for advanced disease is around 12 months [7]. In this scenario, targeted therapies which might overcome the limitations of current treatments are eagerly awaited [8]. Different signaling pathways involved in sarcoma genesis have been investigated so far. Targeting therapies involving (i) cell cycle progression, through cell cycle inhibitors (CDKs) [9,10]; (ii) and growth receptors and pro-survival signaling molecules, through tyrosine kinase inhibitors (TKIs) [11], IGFR [12] and mTOR inhibitors [13], have shown efficacy against sarcomas, but only the VEGFR inhibitor pazopanib has reached the prime time [14]. Inhibition of epigenetic regulators [15] and poly-ADP-ribose-polymerase (PARP) inhibitors have also demonstrated promising anti-cancer activity in preclinical and clinical studies [16].

Even if immunotherapy may be considered a new therapeutic path and some clinical trials based on the use of immune checkpoint inhibitors are currently ongoing [17,18], to date, it is not considered a valuable option for most sarcomas. Other clinical trials are investigating strategies based on endogenous, transgenic, or chimeric antigen receptor (CAR)-expressing T cells for the targeting of specific antigens, such as tyrosine-kinase-like orphan receptor 2, CD133, GD-2, Muc1 and CD117 (e.g., NCT03356782, NCT00902044, NCT04995003, NCT01953900) (<https://clinicaltrials.gov/>, accessed on 10 February 2023) [19]. Nevertheless, the effective treatment of advanced disease is an unmet clinical need, and most sarcomas can still be considered incurable. Novel strategies based on new therapeutic targets are highly desirable.

Recently, the AXL receptor has emerged as a promising candidate target for a variety of sarcomas [20–22]. The AXL gene is located on chromosome 19q13.2. It encodes for the protein called AXL (UFO, ARK, Tyro7, or JTK11), a member of the TAM family of tyrosine kinase receptors (RTKs) characterized by an extracellular, transmembrane, and intracellular domain [22]. The extracellular structure consists of two immunoglobulins (Ig-like) and two fibronectin type III (Fro III-like) chains, while the intracellular domain is important for auto-phosphorylation and signaling kinase activity [23]. In normal cells and tissues, AXL regulates cell survival, non-inflammatory clearance of apoptotic cells, natural killer cell differentiation and platelet aggregation. AXL is also expressed in cancer cells and microenvironmental immune cells, including dendritic cells, macrophages, and NK cells. It drives several cellular processes that are critical for the development, growth and spread of tumors, including proliferation, invasiveness and migration, epithelial–mesenchymal transition, angiogenesis, and immune resistance [24–26].

Different therapeutic agents targeting AXL have been recently developed, including: (i) small molecule inhibitors, which block AXL auto-phosphorylation and kinase activities, such as BGB324, presently investigated in phase I/II clinical trials [27]; (ii) anti-AXL monoclonal antibodies (mAbs), such as YW327.6S2, which bind both human and murine AXL [22]; (iii) nucleotide aptamers, such as the RNA aptamer GL21.T [28]; (iv) soluble AXL receptor that acts as a decoy receptor for the AXL ligand GAS6; (v) natural compounds, such as the *Viscum album* (L.) extract [29].

It was also demonstrated that AXL is over-expressed in Kaposi sarcoma and Kaposi sarcoma herpesvirus-transformed endothelial cells. MAb generated to induce AXL degradation inhibited Kaposi-sarcoma-cell invasion in in vitro models and tumor growth in vivo [30]. A subsequent study identified AXL as a potential therapeutic target for Ewing

sarcoma. AXL inhibitors were shown to affect the viability of Ewing sarcoma cells [31]. In addition, a high expression of AXL gene was found in leiomyosarcoma, and its activity was suppressed by two different multi-tyrosine kinase inhibitors (Crizotinib and Foretinib) [20]. Finally, other studies have found that osteosarcoma cells highly express AXL [32], of which the inhibition significantly reduces lung metastases [21]. Despite all these promising findings, an effective anti-AXL treatment is still not available for these aggressive malignancies.

A novel class of non-immunoglobulin, single-domain therapeutic proteins (Pronectins™), based on “antibody mimics” technology, has been just developed with the aim of providing a novel platform for the treatment of various diseases, including cancer. Pronectins™ were isolated from synthetic human libraries, built upon the 14th domain of Fibronectin III (14FN3) scaffold, which is selected by a bioinformatic approach, and on advanced complementarity-determining region (CDR) diversity of more than 25 billion loop sequences [33]. Since Pronectins™ mimic the natural human repertoire, they are poorly immunogenic [34]. Several pharmacological properties are associated to the fibronectin III scaffold, such as high stability, tissue penetration, and low cost of production. Furthermore, they are smaller than a conventional mAb, representing a favorable feature for the local delivery to the solid tumor mass [35]. Starting from Pronectins™, it is possible to generate multimers, fusion proteins, bispecifics or constructs with site-specific modifications for tailored therapy [36]. Bispecific T-Cell Engagers (BTCEs) emerged as a novel promising strategy for hematologic malignancies, but their application in solid tumors is highly challenging, due to the paucity of selective tumor-associated antigens (TAAs) and the struggle in penetrating the solid tumor mass [37]. In this scenario, a Pronectin™-based BTCE (pBTCE) can help overcome these limitations.

Based on this rationale, we investigated the *in vitro* and *in vivo* activity of a first-in-class pBTCE targeting AXL (pAXL×CD3ε) as a potential immunotherapeutic agent for the treatment of sarcomas.

## 2. Materials and Methods

### 2.1. Generation and Development of pAXL×CD3ε

A highly specific anti-AXL Pronectin™, a non-immunoglobulin and single-domain protein, has been isolated from synthetic libraries based on the human scaffold of the 14th domain of fibronectin III (14FN3), as previously described [38]. By bioinformatic analysis aimed to select the best candidate within the amino acid loop diversity and minimize or prevent immunogenicity, 6 Pronectins™ with a KD < 10 nM were identified and AXL54 was chosen for targeting purposes (KD = 8 nM). This Pronectin™ was used to develop a first-in-class BTCE (AXL54 (Pronectin™)-linker-scFV CD3, pAXL×CD3ε), for investigation as an anti-tumor novel agent. The linker is made of a single unit of Gly4–Ser (GGGS) [38].

### 2.2. Cell Lines

CAL-72, ESS-I, HT-1080, SAOS-2 and Rh-30 were purchased by DSMZ. SW982 and RD-ES were purchased from ATCC. ESS-I (endometrial stromal sarcoma), SAOS-2 (osteogenic sarcoma), SW982 (synovial sarcoma) and RD-ES (Ewing’s sarcoma) were grown in RPMI 1640 (Gibco®, Thermo Fisher Scientific, Waltham, MA, USA), supplemented with 20% fetal bovine serum (FBS) (Lonza Group Ltd., Basel, Switzerland), penicillin (100 U/mL) and streptomycin (100 µg/mL) (Gibco®, Thermo Fisher Scientific). Rh-30 (rhabdomyosarcoma) was cultured in RPMI 1640, supplemented with 10% FBS, 100 U/mL penicillin and 100 µg/mL streptomycin. CAL-72 (osteosarcoma) and HT-1080 (fibrosarcoma) cell lines were cultured in DMEM-GlutaMAX™ (Gibco®, Thermo Fisher Scientific), respectively, supplemented with 20% FBS and 10% FBS, 100 U/mL penicillin and 100 µg/mL streptomycin. Cell lines were maintained at 37 °C, in a humidified atmosphere with 5% CO<sub>2</sub>.

### 2.3. Transduction of Sarcoma Cell Lines

Sarcoma cells were plated at  $1 \times 10^5$  cells/mL in 6-well plate and incubated O/N. To obtain sarcoma cells stably expressing green fluorescent protein (GFP) transgene, a lentiviral GFP-encoding vector was added according to the manufacturer's instruction (SBI System Biosciences, Mountain View, CA, USA). Polybrene (Sigma-Aldrich, Saint Louis, MO, USA) was also used to a final concentration of 8  $\mu\text{g}/\text{mL}$ . Two days after transduction, cells were selected using DMEM, supplemented with 20% FBS, containing 1 mg/mL puromycin (Sigma Aldrich). After antibiotic selection, puromycin-resistant transduced cells were assessed for the expression of GFP by flow cytometry, using Attune NxT Flow cytometer (Thermo Fisher Scientific) and microscopy (Thunder Imaging Systems, Leica Microsystems, Wetzlar, Germany).

### 2.4. Peripheral Blood Mononuclear Cell (PBMC) Isolation

Mononuclear cells were obtained from healthy donor buffy coats. Briefly, PBMCs were isolated by Ficoll-Paque Plus (Cytiva Europe GmbH, Buccinasco, Milan, Italy) density gradient centrifugation, according to the manufacturer's recommendations, and washed twice in the culture medium (RPMI-1640 supplemented with 10% FBS), as previously described [39,40].

### 2.5. Detection of AXL Expression and Target Quantification

AXL expression was analyzed on each sarcoma cell line by flow cytometry. Cells were incubated with FITC-conjugated AXL antibody (#MAB154-100, R&D Systems, Minneapolis, MN, USA) for 15 min at RT in the dark. The tubes were washed in PBS 1X and centrifuged  $400 \times g$  for 5 min, resuspended in 500  $\mu\text{L}$  of PBS 1X and analyzed by a flow cytometer.

To quantify AXL expression on sarcoma cell lines, calibrated microspheres (Quantum Simply Cellular, Bangs Laboratories Inc., Fishers, Castenaso, BO, Italy) were used according to the manufacturer's protocol. Briefly, saturating amounts of FITC-conjugated AXL antibody were added to one drop of each microbead suspension, and the final mixes were incubated for 30 min at RT in the dark. Samples were washed twice using PBS 1X ( $2500 \times g$ ), resuspended in 500  $\mu\text{L}$  of PBS 1X and analyzed by a flow cytometer. Simultaneously, each cell line was stained with FITC-conjugated AXL antibody, as previously described. The analysis was performed maintaining the same instrument setting used for QSC beads. A QuickCal<sup>®</sup> spreadsheet, provided by Bangs Laboratories, was used to convert the main fluorescence intensity (MFI) from microspheres to antibody-binding capacity (ABC) values.

### 2.6. Redirected T-Cell Cytotoxicity Assay

PBMCs were isolated from at least 3 donors and labeled with CellTrace<sup>™</sup> Violet viable marker (Invitrogen, Waltham, MA, USA), according to the manufacturer's instructions, and co-cultured with sarcoma cell lines (CAL-72, ESS-I, HT-1080, SAOS-2, Rh-30, SW982 or RD-ES) at different effector-to-target-cell (E:T) ratio, in the presence of increasing concentrations of pAXL $\times$ CD3 $\epsilon$  (0.1  $\mu\text{g}/\text{mL}$ , 1  $\mu\text{g}/\text{mL}$  and 2.5  $\mu\text{g}/\text{mL}$ ) or anti-B-cell maturation antigen (BCMA) Pronectin<sup>™</sup>-based BTCE, pBCMA $\times$ CD3 $\epsilon$  (2.5  $\mu\text{g}/\text{mL}$ ), as a negative control. BCMA is in fact highly restricted to hematopoietic B cells and is not expressed by solid tumors, therefore representing a suitable negative control in our case. Cells were incubated for 72 h at 37 °C and 5% CO<sub>2</sub>, and finally stained with 7-AAD (BD Biosciences, La Jolla, CA, USA). The cytotoxic effect on sarcoma cell lines was detected by flow cytometry and reported as the percentage of 7-AAD<sup>+</sup>/CellTrace<sup>™</sup> Violet<sup>-</sup> cells. The 10:1 E:T ratio was selected because it allowed for the highest toxicity.

Cells stably expressing GFP gene were co-cultured with PBMCs from at least 3 donors at 10:1 E:T ratio, in the presence of pAXL $\times$ CD3 $\epsilon$  (2.5  $\mu\text{g}/\text{mL}$ ). Cells were incubated for 72 h at 37 °C and 5% CO<sub>2</sub>. Cytotoxicity was assessed by flow cytometry monitoring MFI in GFP-positive cells.

For microscope imaging, co-cultured cells were plated on a round cover glass (Fisher Scientific) above 24 wells, and fixed using 4% paraformaldehyde (PFA) for 15 min. Sections

were washed three times with PBS 1X, mounted in Vectashield with DAPI (Vector Lab, Newark, CA, USA) and analyzed using Thunder Imaging Systems (Leica, Wetzlar, Germany).

### 2.7. Cell Viability Assay

Cells were plated in 96 wells treated with different concentrations of pAXL×CD3ε, and cell viability was evaluated by Cell Titer-Glo Luminescent Assay (CTG; Promega, Madison, WI, USA), as previously reported [41].

### 2.8. Western Blot

Whole-cell protein extracts were obtained using NP40 lysis buffer containing Halt Protease and Phosphatase Inhibitor cocktail (Invitrogen, Thermo Fisher Scientific), separated using 4–12% Novex Bis-Tris SDS-acrylamide gels (Invitrogen), and transferred on nitrocellulose membranes (Bio-Rad, Hercules, CA, USA), as previously reported [42]. Nitrocellulose membranes were incubated O/N at 4 °C with primary antibody. In detail, anti-AXL (#4566) by Cell Signaling Technology (Danvers, MA, USA) and anti-GAPDH (sc-25778) by Santa Cruz (Dallas, TX, USA) were used for Western blotting (WB) procedures. The membrane was washed thrice with PBS-Tween and incubated with the secondary antibody (anti-rabbit IgG HRP-linked antibody #7074S, Cell Signaling Technology) for 1 h at RT. Chemiluminescence was recorded using SuperSignal West Pico PLUS Chemiluminescent Substrate (Thermo Scientific). Densitometric analysis of blots was performed using LI-COR Image Studio Digits Ver 5.0 (Bad Homburg, Germany).

### 2.9. RNA Isolation and Quantitative Real-Time PCR

The WizPrep™ Total RNA Mini Kit (Wizbiosolutions, Seongnam, South Korea) was used, according to the manufacturer's guidelines, to extract purified RNA from sarcoma cell lines. The RNA quantity and quality were assessed by NanoDrop® (ND-1000 Spectrophotometer). cDNA was obtained from the reverse transcription of total RNA, using the "high-capacity cDNA reverse transcription kit" (Applied Biosystems, Foster City, CA, USA). Taq-Man® assay (Life Technologies, Carlsbad, CA, USA) was used to detect and quantify AXL (Hs01064439\_m1), and GAPDH (Hs03929097\_g1) was considered to normalize the recorded threshold cycle values. qRT-PCR was performed in triplicate and relative expression was obtained through the comparative cross threshold method on a ViiA7 System (Thermo Fisher Scientific, Waltham, MA, USA).

### 2.10. T-Cell Activation

Sarcoma cells lines were co-cultured with PBMCs from at least 3 donors at selected 10:1 E:T ratio in the presence of increasing concentrations of pAXL×CD3ε (0.1 µg/mL, 1 µg/mL, and 2.5 µg/mL) or negative control, and were incubated for 72 h at 37 °C and 5% CO<sub>2</sub>. T cells were stained using anti-human CD4 (SK3) FITC (#345768), CD8 (SK1) APC-Cy7 (#641400), CD25 APC (#555434), CD69 PE (#555531), CD3 (UCHT1) PerCP-Cy5.5 (#560835), CD45 (HI30) BV510 (#563204) and CD107a PE (#555801) (BD Biosciences), for 4 h at 37 °C and 5% CO<sub>2</sub>. T cells were selected as CellTrace™ Violet-positive, gated for CD4-, CD8- or CD3-positive, and CD69-, CD25- or CD107a-positive cells. The intracellular production of cytokines and cytolytic enzymes was investigated adding brefeldin A 10 mg/mL. After 4 h, cells were incubated with surface antibodies and treated using FIX&PERM® kit (Nordic MUBio, Susteren, The Netherlands), according to the manufacturer's guidelines. Subsequently, cells were incubated with anti-TNFα PE-Cy™7 (Mab11) (#560678), anti-IFNγ PE (#559327) and anti-Granzyme B (AlexaFluor®647) (#560212) (BD Biosciences) for 15 min at RT in the dark. Samples were finally washed in PBS 1X and analyzed by a flow cytometer.

### 2.11. Analysis of the Activity of pAXL×CD3ε in Combination with Chemotherapeutic Drugs

SAOS-2 were plated in 24 wells and co-cultured at selected 10:1 E:T ratio with PBMCs from at least 3 donors, labelled with CellTrace™ Violet. Cells were treated with pAXL×CD3ε (1 µg/mL), trabectedin (0.2 nM) or their combination (pAXL×CD3ε + tra-

bectedin). After 72 h of incubation, cells were stained using 7-AAD and analysis of positive cells were performed through flow cytometry.

### 2.12. In Vivo Studies

In vivo experiments were performed according to standard guidelines and approved protocols by the National and Institutional Animal Committee (483/2020-PR, 18 May 2020). Four-to-six-week-old male NSG (NOD.Cg-PrkdcscidIl2rgtm1Wjl/SzJ) mice were purchased from Charles River Laboratories (Wilmington, MA, USA). Animals were regularly monitored and euthanized when signs of disease-related symptoms or graft-versus-host disease (GvHD) developed.

To obtain a subcutaneous (sc) xenografted in vivo model, 10 mice were inoculated in the dorsal right flank with HT-1080 cells ( $3 \times 10^6$ ) resuspended in 100  $\mu$ L of PBS 1X. On day 4,  $10 \times 10^6$  PBMCs from healthy donors were intraperitoneally (ip) injected into each mouse. The same day, mice were randomized in 2 groups (5 mice for each group), and 0.1 mg/kg pAXL $\times$ CD3 $\epsilon$  or vehicle were ip injected for 15 consecutive days. Tumor sizes were measured with a digital caliper. The tumor volume (tv) was calculated using the formula:

$$tv = (W^2 \times L)/2, \quad (1)$$

where W is the tumor width and L is the tumor length, as previously described [43].

Mice were sacrificed when the tv reached  $>2000 \text{ mm}^3$ . At the time of sacrifice, blood samples were collected. Red blood cell lysis was performed, and cells were stained with anti-human CD45 BV510 and CD3 PerCP-Cy5.5 to evaluate PBMCs engraftment. Explanted tumors were analyzed by WB, as previously described, using anti-caspase-3 (#9668, Cell Signaling Technology) and anti-PARP (#9532, Cell Signaling Technology), and by immunohistochemistry (IHC) using anti-CD3 antibody (#GA503, Agilent Dako, Glostrup, Denmark).

### 2.13. Statistical Analysis

Statistical evaluations were carried out using a parametric Student's *t*-test by the GraphPad software ([www.graphpad.com](http://www.graphpad.com), accessed on 10 February 2023). Graphpad Prism version 6.0 was used to make graphs. Only results with a *p* value  $< 0.05$  were accepted as statistically significant. Each value is reported as the mean of at least 2 experiments  $\pm$  SD/SEM.

## 3. Results

### 3.1. Evaluation of AXL Expression on Sarcoma Cell Lines

To investigate the expression of AXL on sarcoma cells (Figure 1A), we collected a panel of seven human cell lines, including CAL-72 (osteosarcoma), ESS-I (endometrial stromal sarcoma), HT-1080 (fibrosarcoma), SAOS-2 (osteosarcoma), Rh-30 (rhabdomyosarcoma), SW982 (synovial sarcoma) and RD-ES (Ewing's sarcoma). Flow cytometry showed different AXL expression levels on the surface of tumor cells: high expression on CAL-72, ESS-I and HT-1080; intermediate expression on SAOS-2 and Rh-30; and low- or no-expression on SW982 and RD-ES cell lines, respectively (Figure 1B,C). This trend was confirmed performing quantitative analysis of antigen expression density for each cell line, using calibrated microspheres to assess the antibody-binding capacity (ABC). As reported in Figure 1D, AXL expression was in a range between 21,000 and 4200 antigen molecules on CAL-72 and SW982 cells, respectively. Through qRT-PCR analysis, we assessed the AXL mRNA expression in sarcoma cells (Figure 1E). Our findings revealed a different pattern of target expression, which was in accordance with data retrievable by cBioPortal for the Cancer Genomics dataset ([cbioportal.org](http://cbioportal.org), accessed on 10 February 2023) and Cancer Cell Line Encyclopedia (CCLE) dataset (<https://depmap.org/portal/interactive>, accessed on 10 February 2023). Further Western blot analyses were performed to investigate the expression of AXL protein in sarcoma cells, reporting a clear difference in the band intensity between various cell lines (Figure 1F). According to our results, AXL expression is not correlated to specific sarcoma sub-types.

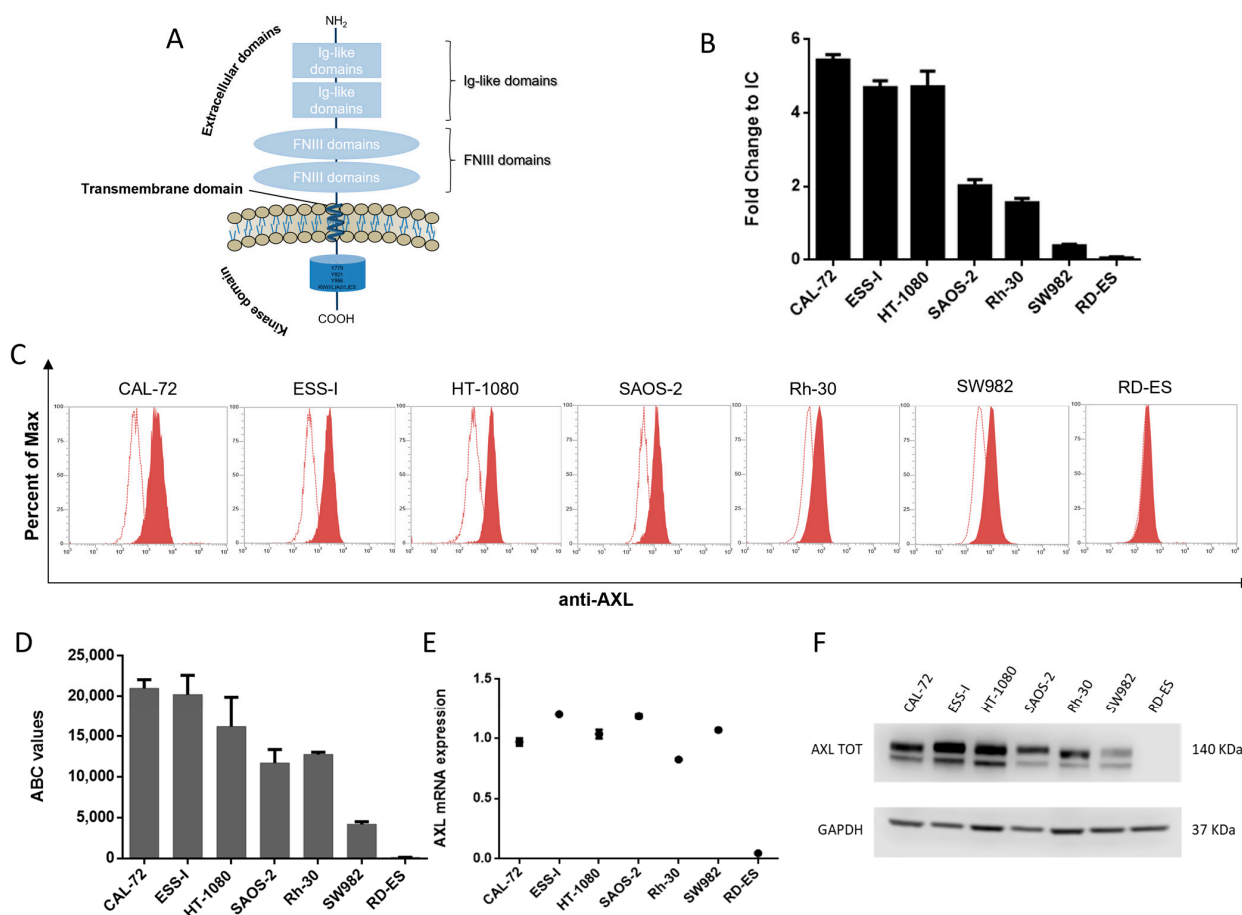


**Figure 1.** AXL expression. (A) Schematic representation of AXL receptor tyrosine kinase structure. It is composed of two immunoglobulin (Ig)-like domains that characterize extracellular domains, two fibronectin type III (FNIII) domains, a transmembrane domain and a kinase domain that is intracellular. (B) Flow cytometry analysis of AXL expression of sarcoma cells. (C) Representative FACS overlays between unstained (empty) and stained (full red) sample of each cell line. (D) Quantification of antibody-binding capacity (ABC) assay. (E) AXL-relative mRNA level determined by qRT-PCR and normalized on GAPDH housekeeping. (F) Western blot of AXL total form reported in a collection panel of sarcoma cells. The uncropped blots are shown in Figure S3.

Our data demonstrate that AXL is highly expressed in sarcoma cells, therefore representing a potential mean for selective targeting. The interaction of pAXL  $\times$  CD3 $\epsilon$  with sarcoma cells was assessed through indirect staining, using an anti-human IgG secondary antibody (Jackson ImmunoResearch, West Grove, PA, USA) (Figure S1).

### 3.2. T-Cell Mediated Cytotoxicity Is Induced by pAXL $\times$ CD3 $\epsilon$ In Vitro

To assess the activity of pAXL  $\times$  CD3 $\epsilon$ , sarcoma cells with different expression levels of AXL were co-cultured with purified human T cells (E:T ratio selected at 10:1) from healthy donors, in the presence of three different concentrations of pAXL  $\times$  CD3 $\epsilon$  (0.1  $\mu$ g/mL, 1  $\mu$ g/mL, and 2.5  $\mu$ g/mL) for 72 h. Increasing concentrations of pAXL  $\times$  CD3 $\epsilon$  produced T-cell-mediated cytotoxicity on sarcoma cells except for the RD-ES because of its low expression of the target antigen (Figure 2A,B). In particular, the cytotoxic activity of pAXL  $\times$  CD3 $\epsilon$  followed a binding-response effect leading to around 50% of cell death on CAL-72, Rh-30, and HT-1080, 40% on SAOS-2, 30% and 20% in SW982 and ESS-1, respectively, at 2.5  $\mu$ g/mL. As a negative control, we performed a cytotoxicity assay using a Pronectin<sup>TM</sup>-based BTCE binding a different target expressed by B cells only, the BCMA, not expressed by sarcoma cells (pBCMA  $\times$  CD3 $\epsilon$ ).

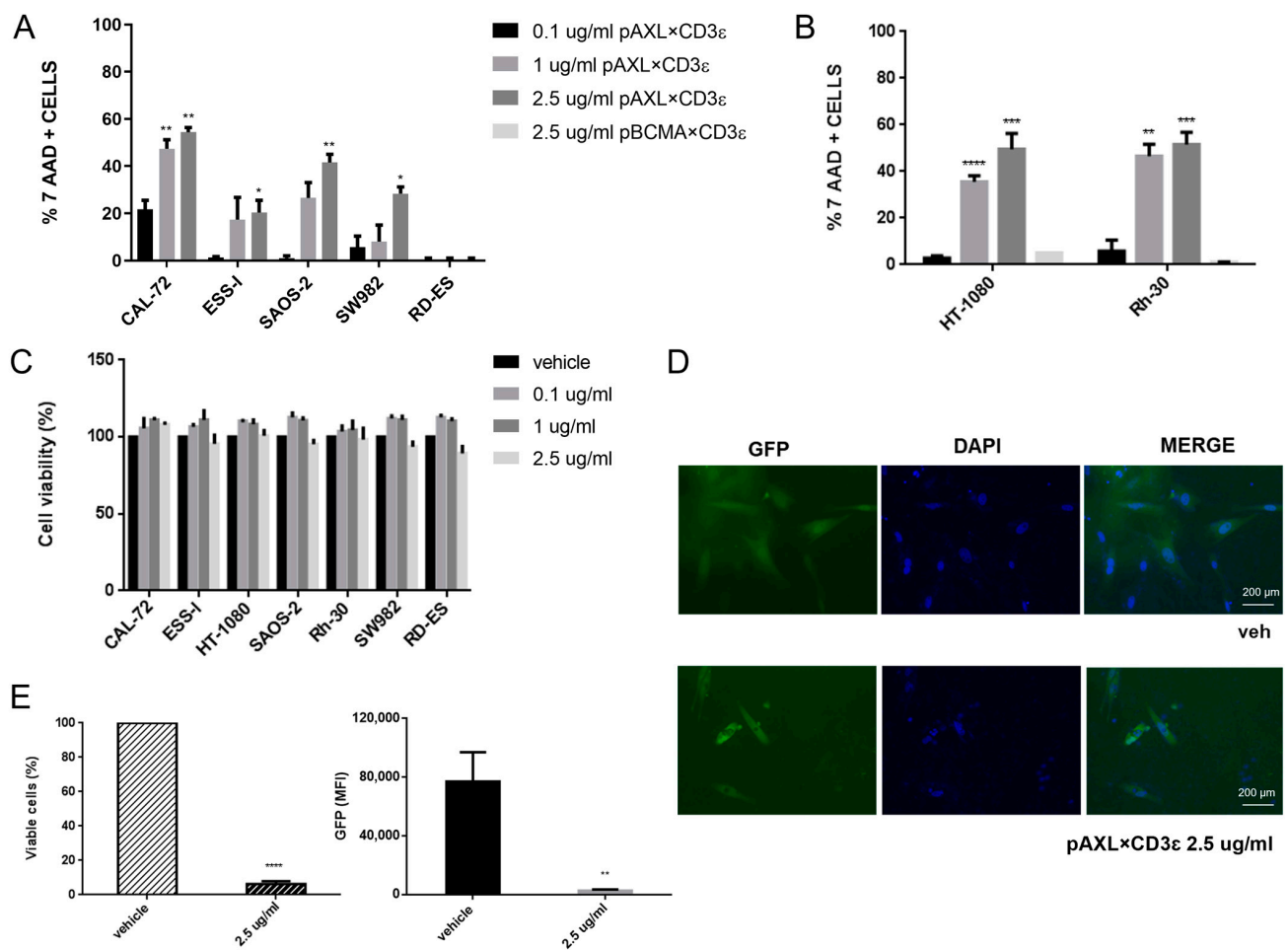


**Figure 2.** Redirected T-lymphocyte cytotoxicity by pAXL×CD3ε in sarcoma cell lines. (A) FACS analysis of 7-AAD(7-amino-actinomycin D)-positive cells. (B) HT-1080 and Rh-30 treated with increasing concentrations of pAXL×CD3ε (0.1 µg/mL, 1 µg/mL and 2.5 µg/mL), and as a negative control 2.5 µg/mL of pBCMA×CD3ε after 72 h. Each group has been compared to the 0.1 µg/mL group for statistical analysis. Results are normalized to the recorded vehicle values. (C) Cell Titer-Glo luminescent cell viability (%) assay performed on sarcoma cell lines without effector cells, following pAXL×CD3ε 72 h treatment. (C) Positive cells (relative percentage %) of sarcoma cell lines co-cultured with peripheral blood mononuclear cells (PBMCs) and treated with different concentrations of pAXL×CD3ε or vehicle for 72 h. Each group has been compared to the 0.1 µg/mL group for statistical analysis. Results are normalized to the recorded vehicle values. (D) Imaging of CAL-72 stably expressing green fluorescent protein (GFP) in untreated cells (vehicle) and 2.5 µg/mL of pAXL×CD3ε-treated cells after 72 h. Nuclei were stained with DAPI and microscopies were performed at 10-fold magnification. (E) Percentage of stably expressing CAL-72 GFP viable cells and median fluorescence intensity (MFI) of GFP analyzed by flow cytometry. PBMCs were obtained from 3 healthy donors and results are expressed as the mean value of triplicate experiments from each donor. \*  $p < 0.0332$ ; \*\*  $p < 0.0021$ ; \*\*\*  $p < 0.0002$ ; \*\*\*\*  $p < 0.0001$ .

As shown in Figure 2B, 2.5 µg/mL of pBCMA×CD3ε did not induce cytotoxicity in two different sarcoma cell lines, such as HT-1080 and Rh-30, when it was used at a higher dose. To exclude direct cytotoxicity of pAXL×CD3ε on sarcoma cells, we performed a cell viability assay that allows the evaluation of metabolically active cells, in the absence of effector cells. We found that different concentrations of pAXL×CD3ε did not alter cell growth capability of cancer cells (Figure 2C), indicating that T lymphocytes are indeed required to induce the redirected cytotoxicity of sarcoma cell lines. Furthermore, we performed co-culture experiments on sarcoma cells stably expressing GFP in the presence of 2.5 µg/mL

of pAXL×CD3ε. As expected, we observed a strong reduction of GFP signal via imaging analysis, confirming the cytotoxic activity of pAXL×CD3ε observed in our experimental models (Figures 2D and S2A). Moreover, the percentage of viable cells and fluorescence quantification evaluated by flow cytometry led to the same result (Figures 2E and S2B).

Taken together, our findings demonstrate that pAXL×CD3ε has an antitumor effect through the recruitment of cytotoxic T lymphocytes.

### 3.3. pAXL×CD3ε Triggers T-Lymphocyte Activation against Sarcoma Cells

Functional effects on PBMCs co-cultured with sarcoma cells at 10:1 E:T ratio, in the presence of increasing concentrations of pAXL×CD3ε or vehicle, were also evaluated after 72 h of treatment. As shown in Figure 3, we observed the upregulation of early and late T-cell surface activation markers (CD69 and CD25) in experiments performed in three different sarcoma cell lines, such as Rh-30, HT-1080 and CAL-72. Additionally, pAXL×CD3ε induced the release of inflammatory cytokine Interferon-γ (IFN-γ) and cytolytic enzyme, Granzyme B.

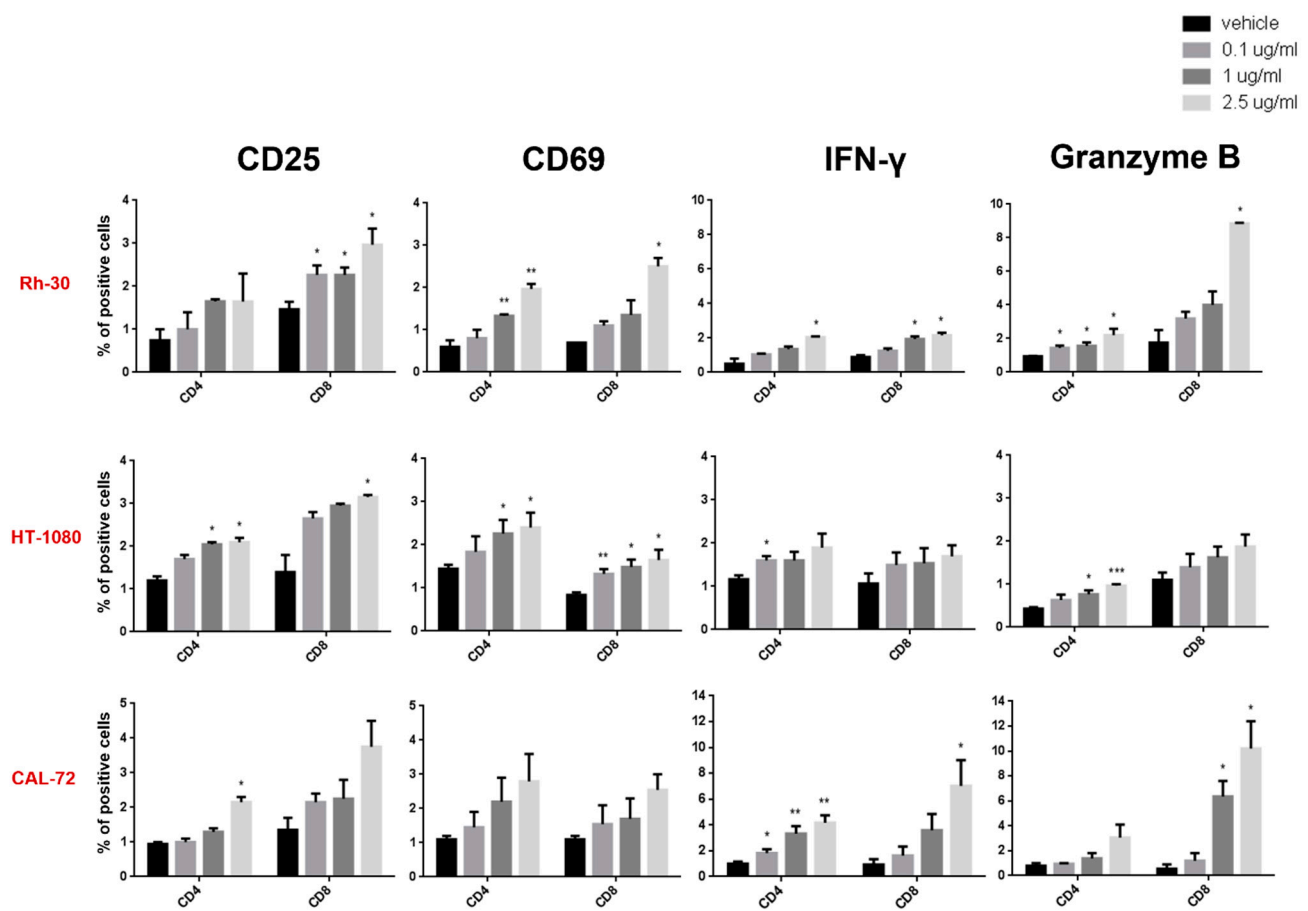


**Figure 3.** Functional experiments on CD4–CD8 gated T cells. Surface early and late activation markers (CD69 and CD25), cytokine release (IFN-γ) and cytolytic enzyme (Granzyme B) on CD4 and CD8-positive T lymphocytes from at least 3 donors co-cultured with Rh-30, HT-1080 and CAL-72 sarcoma cell lines at 10:1 E:T ratio, in the presence of different concentrations of pAXL×CD3ε. Each result is expressed as the mean value of triplicate experiments obtained from each donor. \*  $p < 0.0332$ ; \*\*  $p < 0.0021$ ; \*\*\*  $p < 0.0002$ .

Consistent with their cytotoxic function, T lymphocytes were also positive for CD107a degranulation marker (Figure 4A,B).

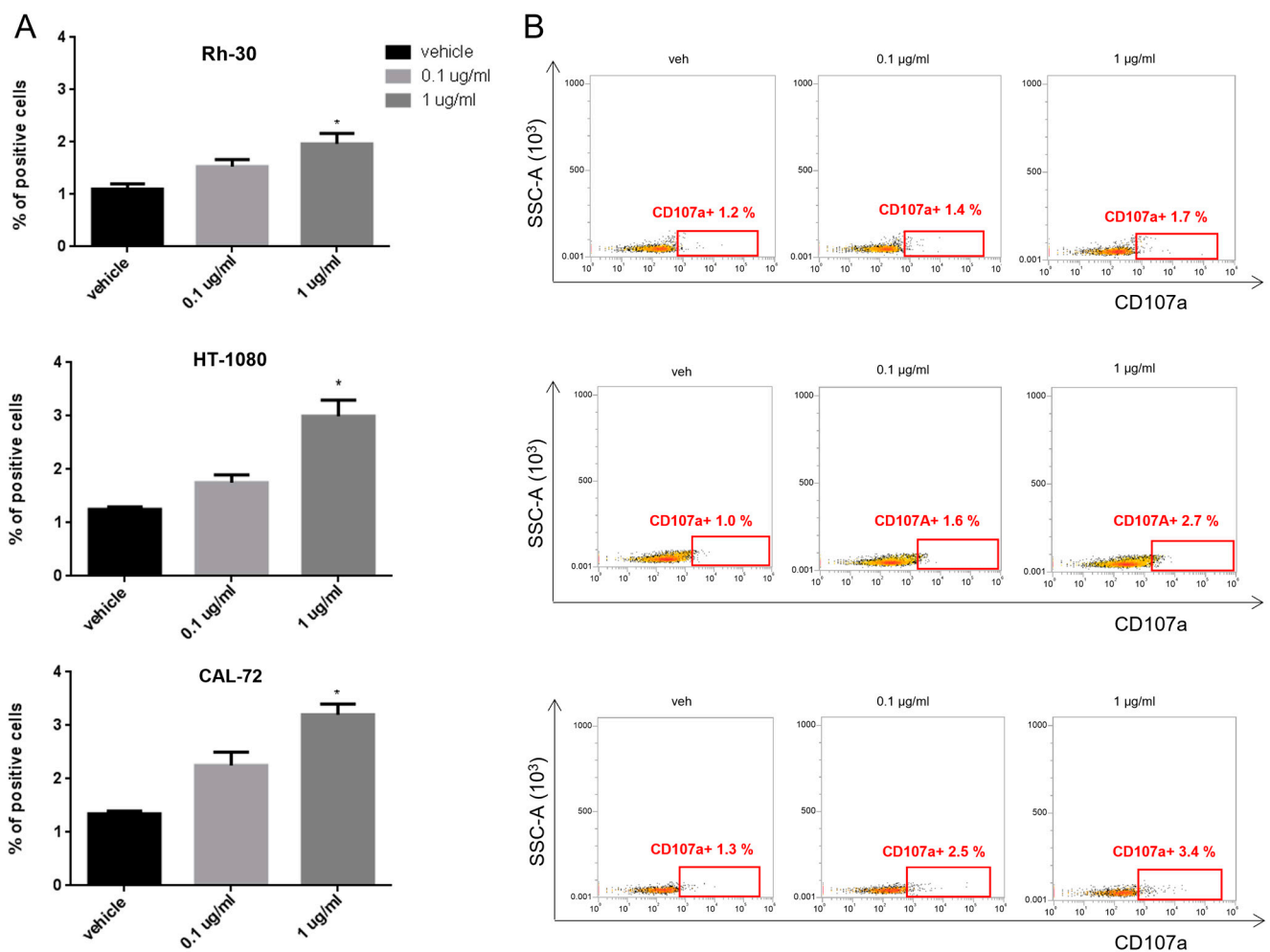


**Figure 4.** Degranulation assay on activated T lymphocytes. **(A)** Histogram quantification of CD107a-positive T cells from at least 3 donors, co-cultured with Rh-30, HT-1080 and CAL-72 sarcoma cell lines and treated with 0.1  $\mu\text{g/ml}$  and 1  $\mu\text{g/ml}$  of pAXL $\times$ CD3 $\epsilon$  for 72 h. **(B)** Representative dot plots of CD107a-positive T lymphocytes analyzed by flow cytometry. Each result is expressed as the mean value of triplicate experiments obtained from each donor. \*  $p < 0.0332$ .

These data indicate that pAXL $\times$ CD3 $\epsilon$  produces a dose-dependent activation of T lymphocytes against AXL-positive sarcoma cells.

### 3.4. pAXL $\times$ CD3 $\epsilon$ Increases Cytotoxicity Induced by Trabectedin

To verify if pAXL $\times$ CD3 $\epsilon$  could make tumor cells more sensitive to conventional chemotherapeutic drugs, SAOS-2 was selected as the cell model to investigate the effect of redirected T-cell toxicity. Cells were co-treated with pAXL $\times$ CD3 $\epsilon$  (1  $\mu\text{g/ml}$ ) and trabectedin (0.2 nM). After 72 h of treatment, an enhanced cytotoxic effect was observed for pAXL $\times$ CD3 $\epsilon$  plus trabectedin, as compared to the effect induced by the single agents. In detail, pAXL $\times$ CD3 $\epsilon$  increased cell death >20% in SAOS-2 cells compared to the effect induced by trabectedin alone (Figure 5A). The dot plots in Figure 5B provide a graphical overview of the reduction in cell viability (%). These data suggest a potential advantage induced by the combination of pAXL $\times$ CD3 $\epsilon$  with chemotherapeutics commonly used for sarcoma therapy.

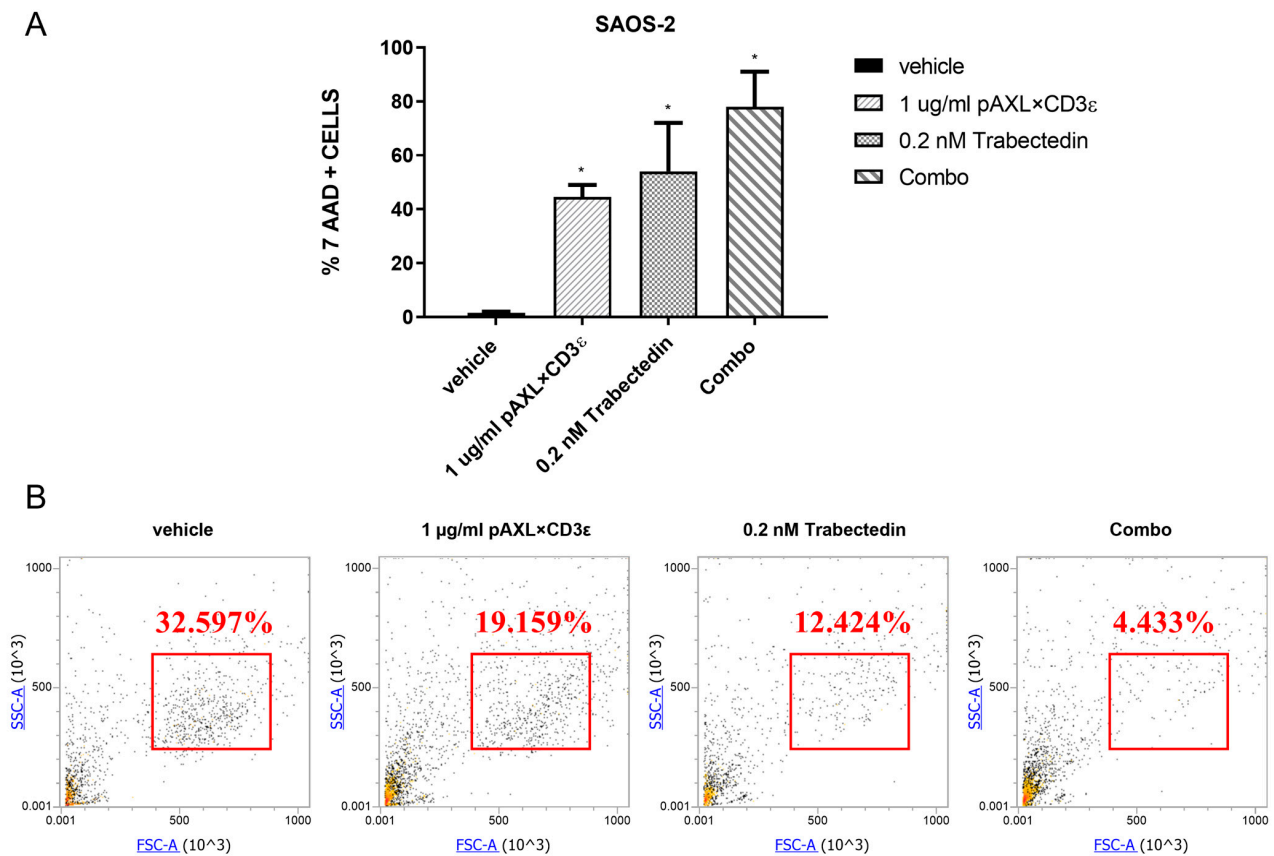


**Figure 5.** pAXL×CD3ε sensitizes chemotherapeutic drug activity in vitro. **(A)** Redirected cytotoxicity T-cell of pAXL×CD3ε in SAOS-2, analyzed in co-culture experiments using 1 µg/mL of pAXL×CD3ε, 0.2 nM of trabectedin and their combination (Combo) for 72 h. **(B)** Representative dot plots of SAOS-2 viability reduction (%) after treatment with pAXL×CD3ε and trabectedin alone or in combination. PBMCs were obtained from 3 healthy donors and results are expressed as the mean value of triplicate experiments from each donor. \*  $p < 0.0332$ .

### 3.5. pAXL×CD3ε In Vivo Activity

The in vivo antitumor efficacy of pAXL×CD3ε was validated against human HT-1080 cell xenografts in NSG-immunocompromised mice (Figure 6A). A total of 10 xenografted mice were randomized to receive pAXL×CD3ε (0.1 mg/kg, five mice) or the vehicle alone (VEH, five mice) as the control group. A significant reduction of tumor growth was observed in NSG mice treated with pAXL×CD3ε as compared to VEH (Figure 6B). After 20 days from the cell engraftment, mice treated with pAXL×CD3ε showed a tumor volume of about 630 mm<sup>3</sup> versus 1200 mm<sup>3</sup> in the VEH-only group. This effect translated into a prolonged survival of treated animals (Figure 6C). To demonstrate the engraftment of human T-lymphocytes in these immunocompromised mice, flow cytometry analyses were performed on peripheral blood samples collected from mice on the day of sacrifice. An anti-CD3-fluorochrome-conjugated antibody was used for the staining, and T-cell engraftment was confirmed both in pAXL×CD3ε and VEH groups (Figure 6D). Retrieved xenografts from mice were homogenized and WB analysis was performed on the whole-cell protein extracts. The analysis revealed the induction of apoptotic processes, which was demonstrated by the increase of cleaved PARP and cleaved caspase-3 in treated mice as compared to VEH (Figure 6E). IHC analyses also highlighted the infiltration of CD3+ cells in tumor xenografts from mice treated with pAXL×CD3ε, thus demonstrating the effective engagement of T-lymphocytes at the tumor site (Figure 6F).

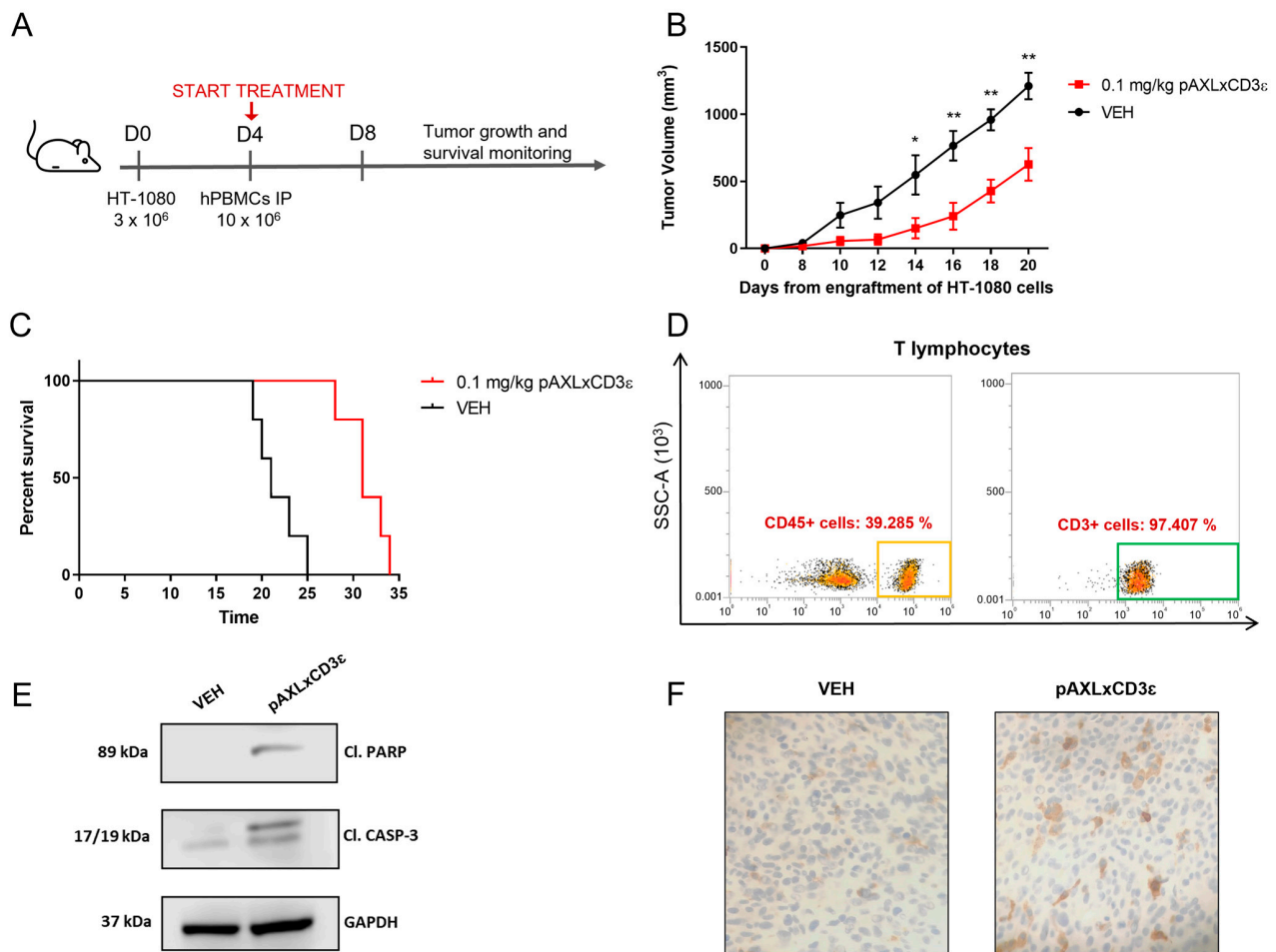


**Figure 6.** pAXL×CD3 $\epsilon$  in vivo activity. (A) Experimental timeline of in vivo study on a sarcoma xenograft model. (B) Tumor volume curve of mice treated with pAXL×CD3 $\epsilon$  0.1 mg/kg or vehicle alone. Results obtained from each group have been compared at the same timepoint for statistical purposes. (C) Survival curves (Kaplan–Meier) of mice treated with pAXL×CD3 $\epsilon$  or vehicle. (D) Representative FACS dot plots of T-cell engraftment evaluated on the day of sacrifice on intracardiac blood samples collected from mice. CD3-positive cells were evaluated on gated CD45-positive lymphocytes. (E) WB analysis of cleaved caspase-3 and cleaved PARP in whole-cell protein extracts from representative retrieved xenografts. GAPDH was used as a loading control. The uncropped blots are shown in Figure S3. (F) IHC staining of CD3 lymphocytes performed on tumors explanted from mice treated with vehicle or pAXL×CD3 $\epsilon$  0.1 mg/kg at 20-fold magnification. \*  $p < 0.0332$ ; \*\*  $p < 0.0021$ .

Based on these findings, pAXL×CD3 $\epsilon$  demonstrates promising antitumor activity against sarcoma xenografts in vivo.

#### 4. Discussion

Cancer immunotherapy based on T-cell engagement is a valuable therapeutic option and is in an advanced phase of clinical evaluation for different hematological malignancies [44–46]. While conventional mAbs bind the same antigen with both fragment antigen-binding (Fab) arms [47], BTCEs simultaneously bind a TAA on cancer cells and the epsilon ( $\epsilon$ ) subunit of CD3 on the T lymphocytes and, therefore, can efficiently trigger redirected T-cell cytotoxicity in an MHC-independent fashion [48,49]. This simultaneous engagement of the antigen on tumor cells and effector cells leads to an immunological synapse, resulting in T-cell activation and subsequent release of inflammatory cytokines and cytolytic molecules that lead to the killing of cancer cells [39,40,50].

Despite their demonstrated efficacy in patients with hematological malignancies, no BTCEs have been approved so far for the treatment of solid tumors [51]. There are, in fact, some main hurdles that can hamper the use of BTCEs in solid tumors: (i) on-target off-tumor toxicities due to the absence of specific TAAs; (ii) impaired anti-cancer activity due to the hostile and immunosuppressive tumor microenvironment (TME) that antagonizes T-cell infiltration into the tumor mass; (iii) reduced bioavailability and scarce penetration within a solid tumor mass [52,53]. In this scenario, the TME may play a relevant role in cancer progression and can influence the clinical management of these diseases [54–56], since it includes immune cells and stromal cells interacting with malignant cells through contact mechanisms or cytokines and subcellular structures, inducing both pro-tumor and antitumor activity. Among them, CD4+ and CD8+ T cells, together with NK cells, dendritic cells, and M1 tumor-associated macrophages (TAMs), promotes cell killing [57–59]. Novel approaches would aim to restore the immune function overcoming cancer suppressive effects [60]. In this light, different strategies are emerging by innovative protein-based scaffolds and novel targets [39,40,61].

Here, we assessed that AXL is highly expressed among a variety of sarcomas, confirming previous data performed on primary sarcoma samples [20,22,31,32,62,63] and representing a promising target for the development of innovative immunotherapeutic approaches, especially in chemo-refractory disease. Previous studies, using mAbs against AXL, have reported activity and manageable toxicity in sarcoma patients, suggesting its targeting potential also in the clinical setting [22,64]. Recently, different strategies based on mAbs and CAR-T cells showed encouraging results against AXL-expressing sarcomas and some of them are currently under clinical investigation. The safety and tolerability of CCT301-38 CAR-modified autologous T cells are being investigated in subjects with r/r sarcomas (NCT05128786). Patients with AXL gene alterations were also recruited for another phase I study to determine the safety, tolerability, pharmacokinetics, and anti-tumor effects induced by Mipasetamab Uzoptirine (ADCT-601) alone, or in combination with other anti-cancer drugs (NCT05389462). The immunogenicity and antitumor efficacy of BA3011, a conditionally active biologic (CAB) AXL-targeted antibody drug conjugate (CAB-AXL-ADC), is being investigated in a phase I/II study in different sarcoma subtypes, in monotherapy or combined with a PD-1 inhibitor (NCT03425279). Finally, a trial has been completed on different tumor types, including sarcoma, to investigate the safety and efficacy of Enapotamab Vedotin (HuMax-AXL-ADC), an AXL-specific antibody drug conjugate (NCT02988817).

On these premises, we focused on AXL as an immunotherapeutic target to be exploited in sarcoma treatment by BTCE-based strategy. We used an emerging protein therapeutic class, called Pronectins™ [36], taking advantage of their small size and low molecular weight to reach a higher concentration within the tumor tissue. Consistently, here we demonstrated that pAXL×CD3ε indeed redirects T cells toward AXL-expressing sarcoma cells, leading to a dose-dependent T-cell activation, with a consequent release of inflammatory cytokines and cytolytic molecules. Our results are in accordance with data recently reported, showing that pAXL×CD3ε exhibits cytotoxic effects on AXL-positive MDA-MB-231 cells and minimal cytotoxicity on AXL-negative CHO cells [38]. Moreover, we found enhanced cytotoxic effects as a function of increased concentrations of pAXL×CD3ε, which was highly promising taking into account the presence of immune cells in the TME of sarcomas. Furthermore, we demonstrated that the combination of pAXL×CD3ε with trabectedin, a conventional active chemotherapeutic drug, improved the cytotoxicity of sarcoma cells. Even if the use of conventional chemotherapeutics is under interindividual variability term of efficacy and toxicity [65–67], our data suggest the feasibility of combinatorial treatments and are consistent with preliminary reports, which showed anti-sarcoma activity of immunotherapy/chemotherapy combination [68]. Importantly, in our *in vivo* model, pAXL×CD3ε guaranteed the recruitment of T lymphocytes in the tumor site and significantly inhibited the growth of sarcoma xenografts, suggesting that this strategy has the potential to also control the fast-growing tumor cells in patients. These findings are of

translational relevance, since conventional approaches are still largely unsuccessful, and the only favorable strategy at the present, for the treatment of this incurable disease, is represented by surgery in combination with pre- or post-surgery therapies.

Overall, we demonstrate that the first-in-class pAXL×CD3ε-based immunotherapy exerts significant anti-sarcoma activity in vitro and in vivo, and therefore represents a promising tool to be developed in the clinical setting, offering a novel opportunity to overcome the unmet need of long-term control of drug refractory disease.

## 5. Conclusions

Despite the identification of molecular mechanisms driving sarcoma genesis, as well as the discovery of key transcription factors, sarcoma treatment still represents a great challenge. The variability in response to current therapies can be ascribed to their heterogeneity and aggressive behavior. Taken together, our results indicate that AXL-targeting by the Pronectin™-based BTCE platform may represent a new-generation strategy for the treatment of this still-incurable disease.

**Supplementary Materials:** The following supporting information can be downloaded at: <https://www.mdpi.com/article/10.3390/cancers15061647/s1>, Figure S1: Interaction of pAXL×CD3ε with sarcoma cells; Figure S2: Redirected T-lymphocyte cytotoxicity by pAXL×CD3ε in sarcoma cell lines; Figure S3: Original Western blots.

**Author Contributions:** N.P., A.M., C.R., D.C., S.S., K.G., S.A. and G.J. performed experiments and/or analyzed the data. C.A.H. and R.C. developed the Pronectin™-based Bispecific T-Cell Engager. F.C. performed IHC analysis. N.S., L.G., M.T.D.M., M.A., G.N. and R.C. provided critical evaluation of experimental data of the manuscript. N.P., A.M., C.R., G.J., P.T. (Pierosandro Tagliaferri) and P.T. (Pierfrancesco Tassone) conceived the study and wrote the manuscript. P.T. (Pierosandro Tagliaferri) and P.T. (Pierfrancesco Tassone) supervised the study. All authors have read and agreed to the published version of the manuscript.

**Funding:** This manuscript has been supported by Institutional funds at Department of Experimental and Clinical Medicine (T27), University Magna Graecia of Catanzaro.

**Institutional Review Board Statement:** The animal study protocol was approved by the Institutional Ethics Committee of Magna Graecia University and all the procedures were performed according to the Institutional Animal-Care-approved protocols and guidelines (483/2020-PR, 18 May 2020).

**Informed Consent Statement:** Not applicable.

**Data Availability Statement:** The data presented in this study are available in this article and Supplementary Materials.

**Acknowledgments:** The authors are grateful to Leonardo Migale for his support in flow cytometry analyses.

**Conflicts of Interest:** R.C. and C.A.H. are associated with Protelica, Inc. that is the owner of Pronectins™ patent. The other authors declare no conflict of interest.

## References

1. Agnoletto, C.; Caruso, C.; Garofalo, C. Heterogeneous circulating tumor cells in sarcoma: Implication for clinical practice. *Cancers* **2021**, *13*, 2189. [[CrossRef](#)] [[PubMed](#)]
2. Siegel, R.L.; Miller, K.D.; Wagle, N.S.; Jemal, A. Cancer statistics, 2023. *CA A Cancer J. Clin.* **2023**, *73*, 17–48. [[CrossRef](#)]
3. Damerell, V.; Pepper, M.S.; Prince, S. Molecular mechanisms underpinning sarcomas and implications for current and future therapy. *Signal Transduct. Target. Ther.* **2021**, *6*, 246. [[CrossRef](#)] [[PubMed](#)]
4. Petrella, A.; Storey, L.; Hulbert-Williams, N.J.; Fern, L.A.; Lawal, M.; Gerrand, C.; Windsor, R.; Woodford, J.; Bradley, J.; O'Sullivan, H. Fear of Cancer Recurrence in Patients with Sarcoma in the United Kingdom. *Cancers* **2023**, *15*, 956. [[CrossRef](#)]
5. Pushpam, D.; Garg, V.; Ganguly, S.; Biswas, B. Management of refractory pediatric sarcoma: Current challenges and future prospects. *OncoTargets Ther.* **2020**, *13*, 5093. [[CrossRef](#)] [[PubMed](#)]
6. Grimer, R.; Judson, I.; Peake, D.; Seddon, B. Guidelines for the management of soft tissue sarcomas. *Sarcoma* **2010**, *2010*, 506182. [[CrossRef](#)] [[PubMed](#)]

7. Italiano, A.; Mathoulin-Pelissier, S.; Cesne, A.L.; Terrier, P.; Bonvalot, S.; Collin, F.; Michels, J.J.; Blay, J.Y.; Coindre, J.M.; Bui, B. Trends in survival for patients with metastatic soft-tissue sarcoma. *Cancer* **2011**, *117*, 1049–1054. [[CrossRef](#)]
8. Evdokimova, V.; Gassmann, H.; Radvanyi, L.; Burdach, S.E. Current State of Immunotherapy and Mechanisms of Immune Evasion in Ewing Sarcoma and Osteosarcoma. *Cancers* **2023**, *15*, 272. [[CrossRef](#)]
9. Kohlmeyer, J.L.; Gordon, D.J.; Tanas, M.R.; Monga, V.; Dodd, R.D.; Quelle, D.E. CDKs in sarcoma: Mediators of disease and emerging therapeutic targets. *Int. J. Mol. Sci.* **2020**, *21*, 3018. [[CrossRef](#)]
10. Thiel, J.T.; Daigeler, A.; Kolbenschlager, J.; Rachunek, K.; Hoffmann, S. The Role of CDK Pathway Dysregulation and Its Therapeutic Potential in Soft Tissue Sarcoma. *Cancers* **2022**, *14*, 3380. [[CrossRef](#)]
11. Wilding, C.P.; Elms, M.L.; Judson, I.; Tan, A.-C.; Jones, R.L.; Huang, P.H. The landscape of tyrosine kinase inhibitors in sarcomas: Looking beyond pazopanib. *Expert Rev. Anticancer. Ther.* **2019**, *19*, 971–991. [[CrossRef](#)] [[PubMed](#)]
12. Guenther, L.M.; Dharia, N.V.; Ross, L.; Conway, A.; Robichaud, A.L.; Catlett, J.L.; Wechsler, C.S.; Frank, E.S.; Goodale, A.; Church, A.J. A Combination CDK4/6 and IGF1R Inhibitor Strategy for Ewing Sarcoma CDK4/6 and IGF1R Inhibitors Are Synergistic in Ewing Sarcoma. *Clin. Cancer Res.* **2019**, *25*, 1343–1357. [[CrossRef](#)]
13. Lim, H.J.; Wang, X.; Crowe, P.; Goldstein, D.; Yang, J.-L. Targeting the PI3K/PTEN/AKT/mTOR pathway in treatment of sarcoma cell lines. *Anticancer. Res.* **2016**, *36*, 5765–5771. [[CrossRef](#)] [[PubMed](#)]
14. Bramwell, V.H. Pazopanib and the treatment palette for soft-tissue sarcoma. *Lancet* **2012**, *379*, 1854–1856. [[CrossRef](#)]
15. Sanaei, M.; Kavooosi, F. Histone deacetylases and histone deacetylase inhibitors: Molecular mechanisms of action in various cancers. *Adv. Biomed. Res.* **2019**, *8*, 63. [[PubMed](#)]
16. Grignani, G.; D'Ambrosio, L.; Pignochino, Y.; Palmerini, E.; Zucchetti, M.; Boccone, P.; Aliberti, S.; Stacchiotti, S.; Bertulli, R.; Piana, R. Trabectedin and olaparib in patients with advanced and non-resectable bone and soft-tissue sarcomas (TOMAS): An open-label, phase 1b study from the Italian Sarcoma Group. *Lancet Oncol.* **2018**, *19*, 1360–1371. [[CrossRef](#)] [[PubMed](#)]
17. Nathenson, M.J.; Conley, A.P.; Sausville, E. Immunotherapy: A new (and old) approach to treatment of soft tissue and bone sarcomas. *Oncologist* **2018**, *23*, 71–83. [[CrossRef](#)]
18. Peterson, C.; Denlinger, N.; Yang, Y. Recent advances and challenges in cancer immunotherapy. *Cancers* **2022**, *14*, 3972. [[CrossRef](#)]
19. Hattinger, C.M.; Patrizio, M.P.; Magagnoli, F.; Luppi, S.; Serra, M. An update on emerging drugs in osteosarcoma: Towards tailored therapies? *Expert Opin. Emerg. Drugs* **2019**, *24*, 153–171. [[CrossRef](#)]
20. Dantas-Barbosa, C.; Lesluyes, T.; Loarer, F.L.; Chibon, F.; Treilleux, I.; Coindre, J.-M.; Meeus, P.; Brahmi, M.; Bally, O.; Ray-Coquard, I. Expression and role of TYRO3 and AXL as potential therapeutic targets in leiomyosarcoma. *Br. J. Cancer* **2017**, *117*, 1787–1797. [[CrossRef](#)]
21. Lamhamedi-Cherradi, S.-E.; Mohiuddin, S.; Mishra, D.K.; Krishnan, S.; Velasco, A.R.; Vetter, A.M.; Pence, K.; McCall, D.; Truong, D.D.; Cuglievan, B. Transcriptional activators YAP/TAZ and AXL orchestrate dedifferentiation, cell fate, and metastasis in human osteosarcoma. *Cancer Gene Ther.* **2021**, *28*, 1325–1338. [[CrossRef](#)] [[PubMed](#)]
22. Zhu, C.; Wei, Y.; Wei, X. AXL receptor tyrosine kinase as a promising anti-cancer approach: Functions, molecular mechanisms and clinical applications. *Mol. Cancer* **2019**, *18*, 153. [[CrossRef](#)] [[PubMed](#)]
23. Kimani, S.G.; Kumar, S.; Bansal, N.; Singh, K.; Kholodovych, V.; Comollo, T.; Peng, Y.; Kotenko, S.V.; Sarafianos, S.G.; Bertino, J.R. Small molecule inhibitors block Gas6-inducible TAM activation and tumorigenicity. *Sci. Rep.* **2017**, *7*, 43908. [[CrossRef](#)] [[PubMed](#)]
24. Goyette, M.-A.; Côté, J.-F. AXL receptor tyrosine kinase as a promising therapeutic target directing multiple aspects of cancer progression and metastasis. *Cancers* **2022**, *14*, 466. [[CrossRef](#)] [[PubMed](#)]
25. Auyez, A.; Sayan, A.E.; Kriaievska, M.; Tulchinsky, E. AXL receptor in cancer metastasis and drug resistance: When normal functions go askew. *Cancers* **2021**, *13*, 4864. [[CrossRef](#)]
26. Wium, M.; Ajayi-Smith, A.F.; Pancez, J.D.; Zerbini, L.F. The role of the receptor tyrosine kinase Axl in carcinogenesis and development of therapeutic resistance: An overview of molecular mechanisms and future applications. *Cancers* **2021**, *13*, 1521. [[CrossRef](#)]
27. Wu, X.; Liu, X.; Koul, S.; Lee, C.Y.; Zhang, Z.; Halmos, B. AXL kinase as a novel target for cancer therapy. *Oncotarget* **2014**, *5*, 9546. [[CrossRef](#)]
28. Cerchia, L.; Esposito, C.L.; Camorani, S.; Rienzo, A.; Stasio, L.; Insabato, L.; Affuso, A.; De Franciscis, V. Targeting Axl with an high-affinity inhibitory aptamer. *Mol. Ther.* **2012**, *20*, 2291–2303. [[CrossRef](#)]
29. Kim, S.; Kim, K.-C.; Lee, C. Mistletoe (*Viscum album*) extract targets Axl to suppress cell proliferation and overcome cisplatin- and erlotinib-resistance in non-small cell lung cancer cells. *Phytomedicine* **2017**, *36*, 183–193. [[CrossRef](#)]
30. Liu, R.; Gong, M.; Li, X.; Zhou, Y.; Gao, W.; Tulpule, A.; Chaudhary, P.M.; Jung, J.; Gill, P.S. Induction, regulation, and biologic function of Axl receptor tyrosine kinase in Kaposi sarcoma. *Blood J. Am. Soc. Hematol.* **2010**, *116*, 297–305. [[CrossRef](#)]
31. Fleuren, E.D.; Hillebrandt-Roeffen, M.H.; Flucke, U.E.; Te Loo, D.M.W.; Boerman, O.C.; van der Graaf, W.T.; Versleijen-Jonkers, Y.M. The role of AXL and the in vitro activity of the receptor tyrosine kinase inhibitor BGB324 in Ewing sarcoma. *Oncotarget* **2014**, *5*, 12753. [[CrossRef](#)] [[PubMed](#)]
32. Han, J.; Tian, R.; Yong, B.; Luo, C.; Tan, P.; Shen, J.; Peng, T. Gas6/Axl mediates tumor cell apoptosis, migration and invasion and predicts the clinical outcome of osteosarcoma patients. *Biochem. Biophys. Res. Commun.* **2013**, *435*, 493–500. [[CrossRef](#)] [[PubMed](#)]
33. Cappuccilli, G.; Crea, R.; Shen, R.; Hokanson, C.A.; Kirk, P.B.; Liston, D.R. Universal Fibronectin Type III Binding-Domain Libraries. U.S. Patent US20090176654A1, 9 July 2009.

34. Chandler, P.G.; Buckle, A.M. Development and differentiation in monobodies based on the fibronectin type 3 domain. *Cells* **2020**, *9*, 610. [[CrossRef](#)] [[PubMed](#)]
35. Lipovšek, D.; Lippow, S.M.; Hackel, B.J.; Gregson, M.W.; Cheng, P.; Kapila, A.; Wittrup, K.D. Evolution of an interloop disulfide bond in high-affinity antibody mimics based on fibronectin type III domain and selected by yeast surface display: Molecular convergence with single-domain camelid and shark antibodies. *J. Mol. Biol.* **2007**, *368*, 1024–1041. [[CrossRef](#)] [[PubMed](#)]
36. Mintz, C.S.; Crea, R. Protein scaffolds: The next generation of protein therapeutics? *Bioprocess Int.* **2013**, *11*, 40–48.
37. Wu, Y.; Yi, M.; Zhu, S.; Wang, H.; Wu, K. Recent advances and challenges of bispecific antibodies in solid tumors. *Exp. Hematol. Oncol.* **2021**, *10*, 56. [[CrossRef](#)]
38. Hokanson, C.A.; Zacco, E.; Cappuccilli, G.; Odineca, T.; Crea, R. AXL-Receptor Targeted 14FN3 Based Single Domain Proteins (Pronectins™) from 3 Synthetic Human Libraries as Components for Exploring Novel Bispecific Constructs against Solid Tumors. *Biomedicines* **2022**, *10*, 3184. [[CrossRef](#)]
39. Caracciolo, D.; Riillo, C.; Ballerini, A.; Gaipa, G.; Lhermitte, L.; Rossi, M.; Botta, C.; Duroyon, E.; Grillone, K.; Cantafio, M.E.G. Therapeutic afucosylated monoclonal antibody and bispecific T-cell engagers for T-cell acute lymphoblastic leukemia. *J. Immunother. Cancer* **2021**, *9*, e002026. [[CrossRef](#)]
40. Riillo, C.; Caracciolo, D.; Grillone, K.; Polerà, N.; Tuccillo, F.M.; Bonelli, P.; Juli, G.; Ascrizzi, S.; Scionti, F.; Arbitrio, M. A Novel Bispecific T-Cell Engager (CD1a × CD3ε) BTCE Is Effective against Cortical-Derived T Cell Acute Lymphoblastic Leukemia (T-ALL) Cells. *Cancers* **2022**, *14*, 2886. [[CrossRef](#)]
41. Grillone, K.; Riillo, C.; Rocca, R.; Ascrizzi, S.; Spanò, V.; Scionti, F.; Polerà, N.; Maruca, A.; Barreca, M.; Juli, G. The New Microtubule-Targeting Agent SIX2G Induces Immunogenic Cell Death in Multiple Myeloma. *Int. J. Mol. Sci.* **2022**, *23*, 10222. [[CrossRef](#)]
42. Neri, P.; Tagliaferri, P.; Di Martino, M.T.; Calimeri, T.; Amodio, N.; Bulotta, A.; Ventura, M.; Eramo, P.O.; Viscomi, C.; Arbitrio, M. In vivo anti-myeloma activity and modulation of gene expression profile induced by valproic acid, a histone deacetylase inhibitor. *Br. J. Haematol.* **2008**, *143*, 520–531.
43. Cosco, D.; Bulotta, A.; Ventura, M.; Celia, C.; Calimeri, T.; Perri, G.; Paolino, D.; Costa, N.; Neri, P.; Tagliaferri, P. In vivo activity of gemcitabine-loaded PEGylated small unilamellar liposomes against pancreatic cancer. *Cancer Chemother. Pharmacol.* **2009**, *64*, 1009–1020. [[CrossRef](#)]
44. Li, L.; Wang, Y. Recent updates for antibody therapy for acute lymphoblastic leukemia. *Exp. Hematol. Oncol.* **2020**, *9*, 33. [[CrossRef](#)] [[PubMed](#)]
45. Topp, M.; Stelljes, M.; Zugmaier, G.; Barnette, P.; Heffner, L.; Trippett, T.; Duell, J.; Bargou, R.; Holland, C.; Benjamin, J. Blinatumomab retreatment after relapse in patients with relapsed/refractory B-precursor acute lymphoblastic leukemia. *Leukemia* **2018**, *32*, 562–565. [[CrossRef](#)]
46. Waldman, A.D.; Fritz, J.M.; Lenardo, M.J. A guide to cancer immunotherapy: From T cell basic science to clinical practice. *Nat. Rev. Immunol.* **2020**, *20*, 651–668. [[CrossRef](#)]
47. Shin, C.; Kim, S.S.; Jo, Y.H. Extending traditional antibody therapies: Novel discoveries in immunotherapy and clinical applications. *Mol. Ther.-Oncolytics* **2021**, *22*, 166–179. [[CrossRef](#)]
48. Slaney, C.Y.; Wang, P.; Darcy, P.K.; Kershaw, M.H. CARs versus BiTEs: A Comparison between T Cell-Redirection Strategies for Cancer Treatment CAR T-cell and BiTE Therapies for Cancers. *Cancer Discov.* **2018**, *8*, 924–934. [[CrossRef](#)]
49. Yu, F.; Gao, Y.; Wu, Y.; Dai, A.; Wang, X.; Zhang, X.; Liu, G.; Xu, Q.; Chen, D. Combination of a Novel Fusion Protein CD3εζ28 and Bispecific T Cell Engager Enhances the Persistence and Anti-Cancer Effects of T Cells. *Cancers* **2022**, *14*, 4947. [[CrossRef](#)] [[PubMed](#)]
50. Wu, Z.; Cheung, N. T cell engaging bispecific antibody (T-BsAb): From technology to therapeutics. *Pharmacol. Ther.* **2018**, *182*, 161–175. [[CrossRef](#)] [[PubMed](#)]
51. Clynes, R.A.; Desjarlais, J.R. Redirected T cell cytotoxicity in cancer therapy. *Annu. Rev. Med.* **2019**, *70*, 437–450. [[CrossRef](#)] [[PubMed](#)]
52. Middelburg, J.; Kemper, K.; Engelberts, P.; Labrijn, A.F.; Schuurman, J.; van Hall, T. Overcoming challenges for CD3-bispecific antibody therapy in solid tumors. *Cancers* **2021**, *13*, 287. [[CrossRef](#)] [[PubMed](#)]
53. Grünewald, T.G.; Alonso, M.; Avnet, S.; Banito, A.; Burdach, S.; Cidre-Aranaz, F.; Di Pompo, G.; Distel, M.; Dorado-Garcia, H.; Garcia-Castro, J. Sarcoma treatment in the era of molecular medicine. *EMBO Mol. Med.* **2020**, *12*, e11131. [[CrossRef](#)] [[PubMed](#)]
54. Deng, J.; Zeng, W.; Kong, W.; Shi, Y.; Mou, X. The study of sarcoma microenvironment heterogeneity associated with prognosis based on an immunogenomic landscape analysis. *Front. Bioeng. Biotechnol.* **2020**, *8*, 1003. [[CrossRef](#)] [[PubMed](#)]
55. Maman, S.; Witz, I.P. A history of exploring cancer in context. *Nat. Rev. Cancer* **2018**, *18*, 359–376. [[CrossRef](#)] [[PubMed](#)]
56. Quail, D.F.; Joyce, J.A. Microenvironmental regulation of tumor progression and metastasis. *Nat. Med.* **2013**, *19*, 1423–1437. [[CrossRef](#)]
57. Ye, H.; Hu, X.; Wen, Y.; Tu, C.; Hornicek, F.; Duan, Z.; Min, L. Exosomes in the tumor microenvironment of sarcoma: From biological functions to clinical applications. *J. Nanobiotechnol.* **2022**, *20*, 403. [[CrossRef](#)]
58. Zhu, S.; Yi, M.; Wu, Y.; Dong, B.; Wu, K. Roles of tumor-associated macrophages in tumor progression: Implications on therapeutic strategies. *Exp. Hematol. Oncol.* **2021**, *10*, 60. [[CrossRef](#)]
59. Mikolajczyk, A.; Mitula, F.; Popiel, D.; Kaminska, B.; Wieczorek, M.; Pieczykolan, J. Two-Front War on Cancer—Targeting TAM Receptors in Solid Tumour Therapy. *Cancers* **2022**, *14*, 2488. [[CrossRef](#)]

60. Clemente, O.; Ottaiano, A.; Di Lorenzo, G.; Bracigliano, A.; Lamia, S.; Cannella, L.; Pizzolorusso, A.; Di Marzo, M.; Santorsola, M.; De Chiara, A. Is immunotherapy in the future of therapeutic management of sarcomas? *J. Transl. Med.* **2021**, *19*, 173. [[CrossRef](#)]
61. Gebauer, M.; Skerra, A. Engineered protein scaffolds as next-generation antibody therapeutics. *Curr. Opin. Chem. Biol.* **2009**, *13*, 245–255. [[CrossRef](#)]
62. Van Renterghem, B.; Wozniak, A.; Castro, P.G.; Franken, P.; Pencheva, N.; Sciot, R.; Schöffski, P. Enapotamab Vedotin, an AXL-Specific Antibody-Drug Conjugate, Demonstrates Antitumor Efficacy in Patient-Derived Xenograft Models of Soft Tissue Sarcoma. *Int. J. Mol. Sci.* **2022**, *23*, 7493. [[CrossRef](#)] [[PubMed](#)]
63. May, C.D.; Garnett, J.; Ma, X.; Landers, S.M.; Ingram, D.R.; Demicco, E.G.; Al Sannaa, G.A.; Vu, T.; Han, L.; Zhang, Y. AXL is a potential therapeutic target in dedifferentiated and pleomorphic liposarcomas. *BMC Cancer* **2015**, *15*, 901. [[CrossRef](#)] [[PubMed](#)]
64. Rios-Doria, J.; Favata, M.; Lasky, K.; Feldman, P.; Lo, Y.; Yang, G.; Stevens, C.; Wen, X.; Sehra, S.; Katiyar, K. A potent and selective dual inhibitor of AXL and MERTK possesses both immunomodulatory and tumor-targeted activity. *Front. Oncol.* **2020**, *10*, 598477. [[CrossRef](#)] [[PubMed](#)]
65. Arbitrio, M.; Di Martino, M.T.; Scionti, F.; Barbieri, V.; Pensabene, L.; Tagliaferri, P. Pharmacogenomic profiling of ADME gene variants: Current challenges and validation perspectives. *High-Throughput* **2018**, *7*, 40. [[CrossRef](#)] [[PubMed](#)]
66. Arbitrio, M.; Scionti, F.; Di Martino, M.T.; Caracciolo, D.; Pensabene, L.; Tassone, P.; Tagliaferri, P. Pharmacogenomics biomarker discovery and validation for translation in clinical practice. *Clin. Transl. Sci.* **2021**, *14*, 113–119. [[CrossRef](#)] [[PubMed](#)]
67. DeRidder, L.; Rubinson, D.A.; Langer, R.; Traverso, G. The past, present, and future of chemotherapy with a focus on individualization of drug dosing. *J. Control. Release* **2022**, *352*, 840–860. [[CrossRef](#)]
68. Engelsen, A.S.; Lotsberg, M.L.; Abou Khouzam, R.; Thiery, J.-P.; Lorens, J.B.; Chouaib, S.; Terry, S. Dissecting the role of AXL in cancer immune escape and resistance to immune checkpoint inhibition. *Front. Immunol.* **2022**, *13*, 869676. [[CrossRef](#)]

**Disclaimer/Publisher’s Note:** The statements, opinions and data contained in all publications are solely those of the individual author(s) and contributor(s) and not of MDPI and/or the editor(s). MDPI and/or the editor(s) disclaim responsibility for any injury to people or property resulting from any ideas, methods, instructions or products referred to in the content.